

NUREG/CR-0409
SUNYSB-NUREG-0011

A STUDY OF DROPLET HYDRODYNAMICS IMPORTANT IN LOCA REFLOOD

Quarterly Progress Report
January 1 - March 31, 1978

R. L. Lee and D. S. Azbel

State University of New York at Stony Brook

Prepared for
U.S. Nuclear Regulatory Commission

7811070333

NOTICE

This report was prepared as an account of work sponsored by the United States Government. Neither the United States nor the United States Nuclear Regulatory Commission, nor any of their employees, nor any of their contractors, subcontractors, or their employees, makes any warranty, express or implied, nor assumes any legal liability or responsibility for the accuracy, completeness or usefulness of any information, apparatus, product or process disclosed, nor represents that its use would not infringe privately owned rights.

Available from
National Technical Information Service
Springfield, Virginia 22161
Price: Printed Copy \$4.50; Microfiche \$3.00

The price of this document for requesters outside of the North American Continent can be obtained from the National Technical Information Service.

NUREG/CR-0409
SUNYSB-NUREG-0011
R4

A STUDY OF DROPLET HYDRODYNAMICS IMPORTANT IN LOCA REFLOOD

Quarterly Progress Report
January 1 - March 31, 1978

Richard S.L. Lee and David S. Azbel

Manuscript Completed: May 1978
Date Published: September 1978

College of Engineering and Applied Sciences
State University of New York at Stony Brook
Stony Brook, NY 11794

Division of Reactor Safety Research
Office of Nuclear Regulatory Research
U.S. Nuclear Regulatory Commission
Under Contract No. NRC-04-78-194

FOREWORD

This second Quarterly Progress Report covers the development work on droplet hydrodynamics important in LOCA reflood performed during the time from January 1, 1978 to March 31, 1978 in the Department of Mechanical Engineering at the State University of New York at Stony Brook, under Contract No. NRC-04-78-194 for the Nuclear Regulatory Commission. The individual contributions by the Stony Brook staff members are indicated in the text.

ABSTRACT

The purpose of the theoretical and experimental work reported here is to investigate the fluid mechanical and heat transfer phenomena that are believed to occur during the reflood portion of the hypothesized LOCA. Particular emphasis is placed on the fluid mechanical aspects in this report and the velocity and size distribution of the water droplets in a turbulent air flow has been simulated.

In the experimental part, the results of the local measurement of turbulent upward flow of a dilute water droplet-air two-phase dispersion in a vertical rectangular channel are presented.

In the theoretical part the results obtained for dilute two-phase (air-water droplets) turbulent flow inside a rectangular channel with film on the wall is analyzed and a model developed.

LIST OF TABLES

<u>SECTION A: FLOW MEASUREMENTS</u>	<u>PAGE</u>
Table 1 - Flow Conditions.	18
<u>SECTION B: MODEL DEVELOPMENT</u>	
Table 1 - Comparison of Measured Droplet Relative Velocity in a Rectangular Channel without Liquid Film on Wall with Corresponding Theoretical Results.	27

LIST OF FIGURES

<u>SECTION A: FLOW MEASUREMENTS</u>	<u>PAGE</u>
<u>FIGURE NO.</u>	
1	Flow Arrangement with Liquid Film on Wall. . . . 7
2	Droplet Size and Number Density Distributions with Liquid Film on Wall (0.25mm from wall). . . 8
3	Droplet Size and Number Density Distributions with Liquid Film on Wall (0.50mm from wall). . . 8
4	Droplet Size and Number Density Distributions with Liquid Film on Wall (1.00mm from wall). . . 8
5	Droplet Size and Number Density Distributions with Liquid Film on Wall (2.00mm from wall). . . 8
6	Droplet Size and Number Density Distributions with Liquid Film on Wall (3.00mm from wall). . . 9
7	Droplet Size and Number Density Distributions with Liquid Film on Wall (4.00mm from wall). . . 9
8	Droplet Size and Number Density Distributions with Liquid Film on Wall (5.00mm from wall). . . 9
9	Droplet Velocity Distributions with Liquid Film on Wall (0.25mm from wall). 9
10	Droplet Velocity Distributions with Liquid Film on Wall (0.50mm from wall). 10
11	Droplet Velocity Distributions with Liquid Film on Wall (1.00mm from wall). 10
12	Droplet Velocity Distributions with Liquid Film on Wall (2.00mm from wall). 10
13	Droplet Velocity Distributions with Liquid Film on Wall (3.00mm from wall). 10
14	Droplet Velocity Distributions with Liquid Film on Wall (4.00mm from wall). 11

<u>FIGURE NO.</u>		<u>PAGE</u>
15	Droplet Velocity Distributions with Liquid Film on Wall (5.00mm from wall)	11
16	Air Velocity Distributions with Liquid Film on Wall	11
17	Sketch of Droplet Entrainment from Liquid Film on Wall.	11
18	Flow Arrangement.	12
19	Droplet Size and Number Density Distributions without Liquid Film on Wall (0.25mm from wall)...	13
20	Droplet Size and Number Density Distributions without Liquid Film on Wall (0.50mm from wall). .	13
21	Droplet Size and Number Density Distributions without Liquid Film on Wall (0.75mm from wall). .	13
22	Droplet Size and Number Density Distributions without Liquid Film on Wall (1.00mm from wall). .	13
23	Droplet Size and Number Density Distributions without Liquid Film on Wall (1.50mm from wall). .	14
24	Droplet Size and Number Density Distributions without Liquid Film on Wall (2.00mm from wall). .	14
25	Droplet Size and Number Density Distributions without Liquid Film on Wall (3.00mm from wall). .	14
26	Droplet Size and Number Density Distributions without Liquid Film on Wall (4.00mm from wall). .	14
27	Droplet Size and Number Density Distributions without Liquid Film on Wall (5.00mm from wall). .	15
28	Droplet Velocity Distributions without Liquid Film on Wall (0.25mm from wall)	15
29	Droplet Velocity Distributions without Liquid Film on Wall (0.50mm from wall)	15
30	Droplet Velocity Distributions without Liquid Film on Wall (0.75mm from wall)	15

<u>FIGURE NO.</u>	<u>PAGE</u>
31	Droplet Velocity Distributions without Liquid Film on Wall (1.00mm from wall). 16
32	Droplet Velocity Distributions without Liquid Film on Wall (1.50mm from wall). 16
33	Droplet Velocity Distributions without Liquid Film on Wall (2.00mm from wall). 16
34	Droplet Velocity Distributions without Liquid Film on Wall (3.00mm from wall). 16
35	Droplet Velocity Distributions without Liquid Film on Wall (4.00mm from wall). 17
36	Droplet Velocity Distributions without Liquid Film on Wall (5.00mm from wall). 17
37	Air Velocity Distributions without Liquid Film on Wall. 17
38	Droplet Distributions without Liquid Film on Wall 17

TABLE OF CONTENTS

	<u>PAGE</u>
FORWARD	iii
ABSTRACT	iv
LIST OF TABLES	v
LIST OF FIGURES	vi
TABLE OF CONTENTS	ix
SECTION A: FLOW MEASUREMENTS	
INTRODUCTION	1
STATUS SUMMARY	1
ACHIEVEMENTS	2
EXPERIMENT 1: MEASUREMENTS IN A RECTANGULAR CHANNEL (with liquid film on wall)	2
EXPERIMENT 2: MEASUREMENTS IN A RECTANGULAR CHANNEL (without liquid film on wall)	5
CONCLUSIONS	6
SECTION B: MODEL DEVELOPMENT	
AN ONE-DIMENSIONAL ANALYSIS OF THE MOTION OF SMALL LIQUID DROPLETS (8-97 μ m) IN THE FLOW OF TWO-PHASE DISPERSION IN A RECTANGULAR VERTICAL DUCT	19
REFERENCES	30

SECTION A: FLOW MEASUREMENTS

(R. S. L. Lee, J. Srinivasan and R. Hitzgrath)

INTRODUCTION

The primary objective of this investigation is to understand droplet hydrodynamics under conditions simulating steam-water droplet flow-- predicted to occur during the reflood portion of LOCA. The results will be used to further substantiate the constitutive equations necessary to predict heat transfer during core reflooding in the vicinity of the rising water level where droplets are formed by violent boiling and broken up by leidenfrost phenomenon. First, this information is obtained by simulating the behavior of the water droplets present during the actual LOCA process in an adiabatic flow inside a simplified test section. To do this, an entirely new methodology and experimental hardware has been developed. This technique has been applied to a solid particulate in water (two phase) system with particle size-density distributions and velocity distributions being obtained using a custom-made laser Doppler anemometer (L.D.A.).

STATUS SUMMARY

A new optical technique using laser-Doppler anemometry has been developed and has been applied to a solid particle-water two-phase flow and a water droplet-air two-phase flow to obtain the local number densities of particles/droplets and two-dimensional velocity probability densities of both homogeneous and dispersed phase. This novel measuring technique,

the accompanying data processing electronic package and the results of these measurements have been presented in Quarterly Report #SUNYSB-NUREG-0001 NRC-04 through Quarterly Report #SUNYSB-NUREG-0009 NRC-04.

This measuring scheme has now been used to study the deposition of water droplets during turbulent flow of air-water droplet flow in a vertical rectangular channel. Measurements have been made both with and without a continuous liquid film on the channel walls. The results of these experiments have been presented at the Two-Phase Flow Instrumentation Review Group Meeting at Troy, New York, February 13-14, 1978 and are explained in the following sections.

ACHIEVEMENTS

A wide band tape-recorder (model 101 - Honeywell) has been received and was used to record high frequency signals--higher axial air-droplet velocities.

The data-processing electronics were also modified to handle high frequency Doppler signals. The droplet-size distribution and velocity distribution has been obtained over the cross section of a rectangular channel with a liquid film build-up present on the channel wall. Also, measurements were made for dilute two-phase turbulent flow inside the rectangular channel without any wall film present.

EXPERIMENT 1: MEASUREMENTS IN A RECTANGULAR CHANNEL (with liquid film on wall)

The flow system was designed to generate a two-phase turbulent flow of water droplets (ranging from submicrons to 100μ in diameter)

in air through a vertical rectangular channel of dimensions 10 mm. x 25 mm. with measurements to be taken at points along the lateral axis across its smaller dimension.

The system consisted of a nozzle supplying water to be atomized by a high velocity annular air jet encircling the nozzle. The droplet generation and turbulent air supply were thus coupled in a device which resembled an ejector pump. The atomizer was aimed at the entrance end of the channel and the whole assembly--the atomizer and the end of the channel--was enclosed in a plexiglass box to collect excess water. To better control droplet size the air supplied to the atomizer was pre-saturated with water to suppress any possible evaporation of the droplets. Also, to control the number of droplets and to limit the size range entering the test section, a thin perforated plate was placed between the atomizing device and the entrance to the channel. A plate with 18-1.5 mm. diameter holes was selected as it provided the necessary control. Finally, to prevent the droplets from falling back into the channel, a jet of air was aimed at the exiting flow so that it blew the droplets away, and yet did not disturb the flow inside the channel. The test section was equipped with two-100 mm. long plate glass observation windows mounted on opposite sides of the rectangular channel near the exit end. An adjustable mounting brace was used so that the test section could be aligned. The glass plates were aligned to be parallel to each other and the entire test section was aligned so that measurements could be made at locations near the wall. The flow arrangement is shown in Figure 1.

The center point of the optical measuring volume was placed at a level of 582 mm. from the channel entrance and measurements were taken successively at nine different lateral positions across the channel. The three analog signals were recorded at each measuring location on over 4000 feet of magnetic tape at a taping speed of 120 inches per second. The tape recorder had a higher frequency response and hence measurements could be made at higher velocities.

The recorded signals were played back at 15 inches per second through the electronic circuits into a PDP-15 digital computer for data analysis. The entire summary of the data analysis is presented in Appendix-1. The measured number densities of the different size droplets at various distances from the wall are shown in Figures 2 to 8. The mean axial and lateral velocity distributions and the standard deviations for droplets at different distances are shown in Figures 9 to 15. Axial and lateral velocities of the air were determined using submicron size droplets. Their distribution is shown in Figure 16.

It was noted in this particular flow that the droplets formed a continuous water film on the wall upstream of the observation section. An analysis of the experimental data revealed that very near the wall (0.25 mm.) there were large droplets (80μ to 95μ). At 0.5 mm. the number of large droplets was less and at 1 mm. the number is smaller droplets increased by at least one order of magnitude. When this was analyzed, taking lateral velocity data into consideration, the following observations were made: There was active generation of large droplets from the wall film. These droplets broke up into a large number of

smaller droplets due to the violent shear flow of air. These small droplets were found to move at higher lateral velocities in the away-from-the-wall direction, and coalesce, forming large droplets at 2 mm. from the wall, and then breakup again into medium-size droplets at 3 mm. from the wall. This is shown in Figure 17.

It was observed that the flow in the channel was unsteady due to the droplet entrainment from the wall film. Hence attempts were made to study the droplet distribution without any wall film.

EXPERIMENT 2: MEASUREMENTS IN A RECTANGULAR CHANNEL (without liquid film on wall)

The flow system was modified to generate a two-phase turbulent flow of water droplets without any visible water film present on the wall. In order to achieve this the following changes were made: The water flow was reduced and the air flow going into the atomizing device was increased. The perforated plate was replaced by a small rectangular orifice. This flow arrangement is shown in Figure 18. The flow conditions for both experiments are listed for comparison in Table 1.

The measuring volume was placed at a level of 5th mm. from the channel entrance and, as before, it was moved along the lateral axis through nine successive measuring locations. The data accumulation and analysis were done using the same procedure outlined for the previous experiment.

The measured number densities of various size droplets at different distances from the wall are shown in Figures 19-27; the droplet velocity distribution and the corresponding standard deviations are shown in Figures

28-36; and the air velocity distributions at different distances from the wall are shown in Figure 37. The data summary for these nine locations is presented in Appendix-2. An analysis of the experimental data revealed some interesting features of the two-phase dispersed flow. The droplets were generally found to lag behind the air flow in the axial direction. The amount of this lagging was found to increase with droplet size. However, in the lateral direction the medium and small sized droplets near the wall were generally found to migrate towards the wall. The response of various size droplets for the same turbulent field was different and hence the number densities of the various size droplets had different distributions and they had a peak at different distances from the wall as shown in Figure 38. Furthermore, the large size droplets above 55μ were not present at the center of the channel.

CONCLUSIONS

The Doppler signals recorded for dilute two-phase (air-water droplet) turbulent flow inside a rectangular channel were analyzed and discussed in this report. The results of the tests at different entrance lengths will be reported in the next quarterly report.

The flow arrangement is being modified to make measurements in a simulated rod bundle test section.

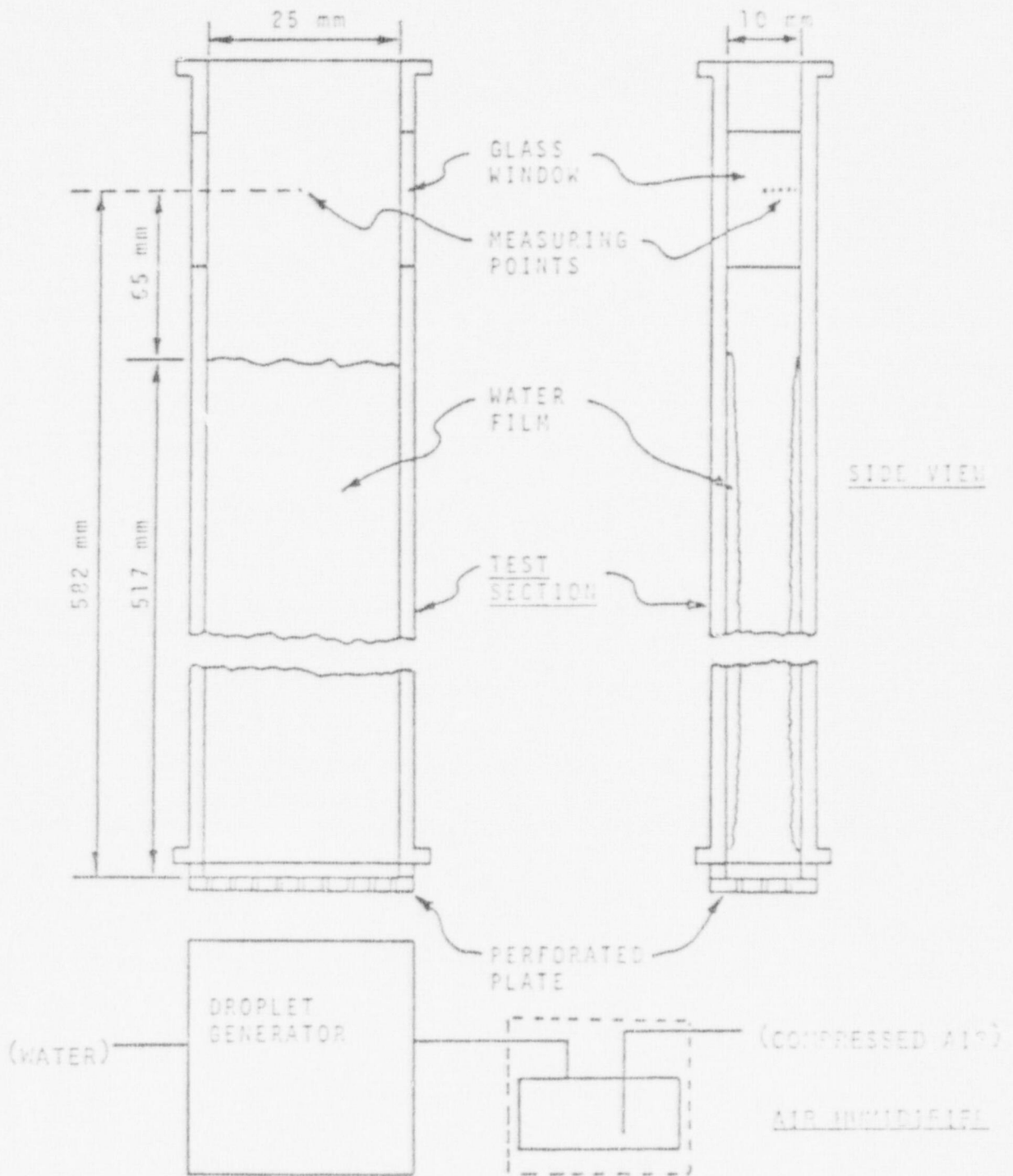


FIGURE 1. FLOW ARRANGEMENT WITH LIQUID FILM ON WALL



FIGURE 2. DROPLET SIZE AND NUMBER DENSITY DISTRIBUTIONS WITH LIQUID FILM ON WALL

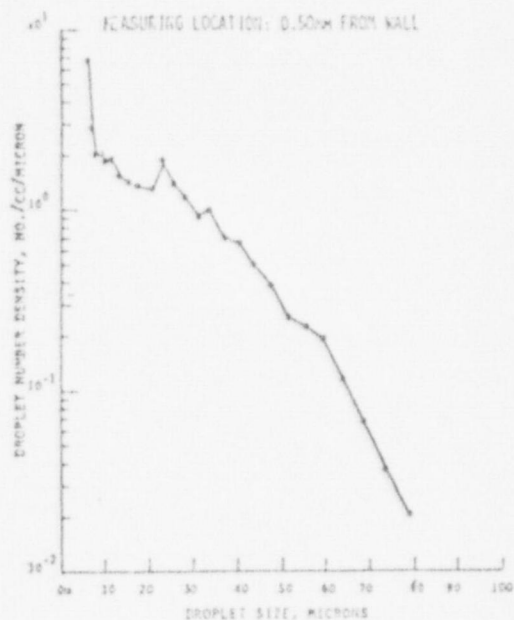


FIGURE 3. DROPLET SIZE AND NUMBER DENSITY DISTRIBUTIONS WITH LIQUID FILM ON WALL



FIGURE 4. DROPLET SIZE AND NUMBER DENSITY DISTRIBUTIONS WITH LIQUID FILM ON WALL

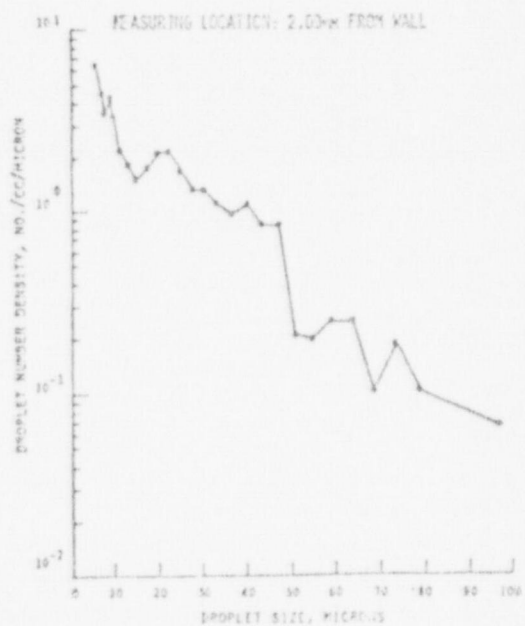


FIGURE 5. DROPLET SIZE AND NUMBER DENSITY DISTRIBUTIONS WITH LIQUID FILM ON WALL

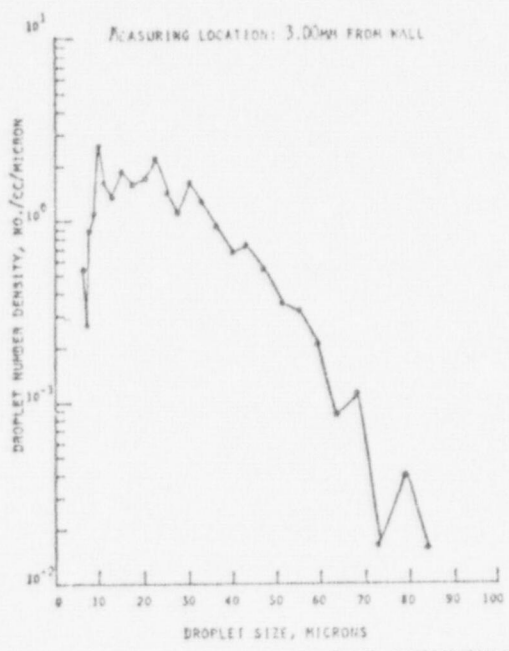


FIGURE 6. DROPLET SIZE AND NUMBER DENSITY DISTRIBUTIONS WITH LIQUID FILM ON WALL

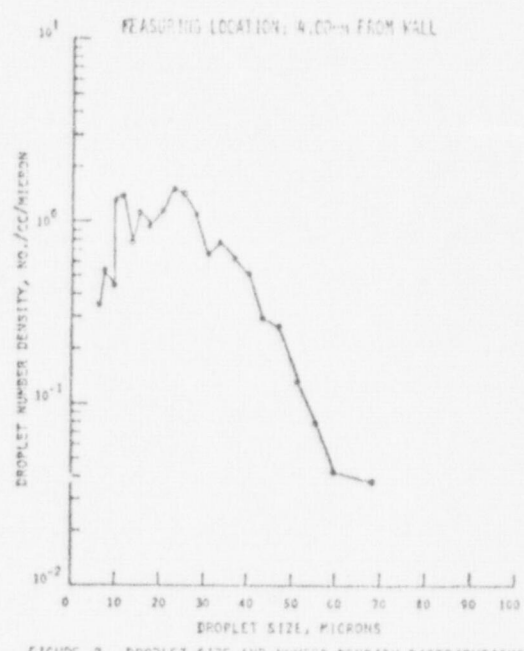


FIGURE 7. DROPLET SIZE AND NUMBER DENSITY DISTRIBUTIONS WITH LIQUID FILM ON WALL

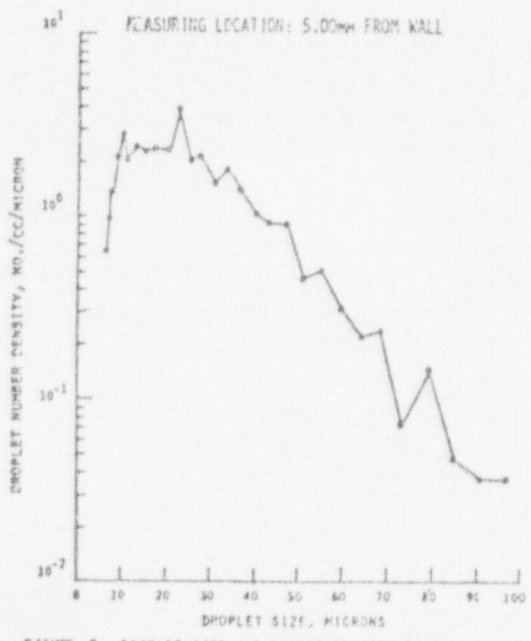


FIGURE 8. DROPLET SIZE AND NUMBER DENSITY DISTRIBUTIONS WITH LIQUID FILM ON WALL

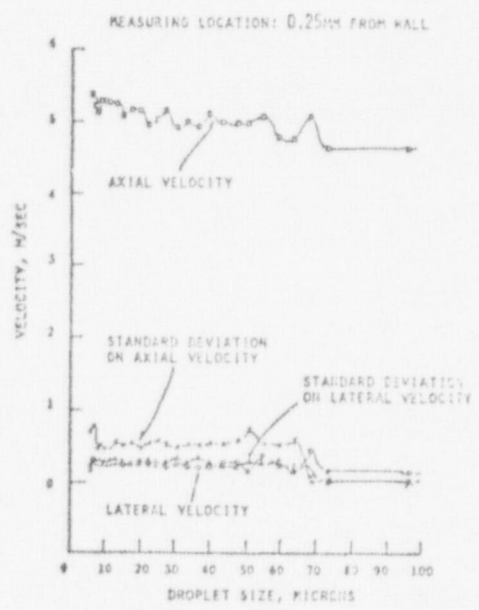


FIGURE 9. DROPLET VELOCITY DISTRIBUTIONS WITH LIQUID FILM ON WALL

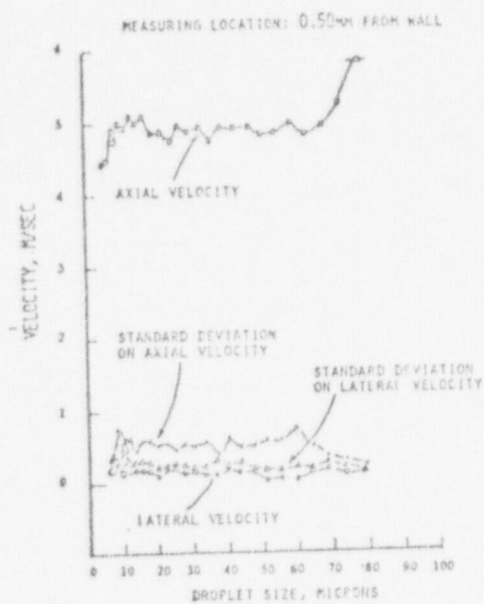


FIGURE 10. DROPLET VELOCITY DISTRIBUTIONS WITH LIQUID FILM ON WALL

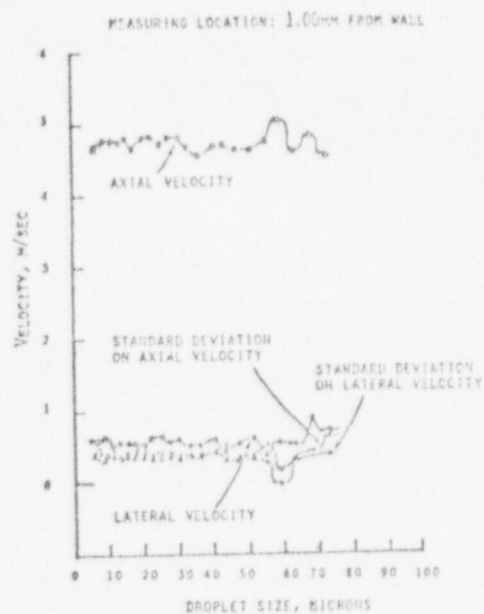


FIGURE 11. DROPLET VELOCITY DISTRIBUTIONS WITH LIQUID FILM ON WALL

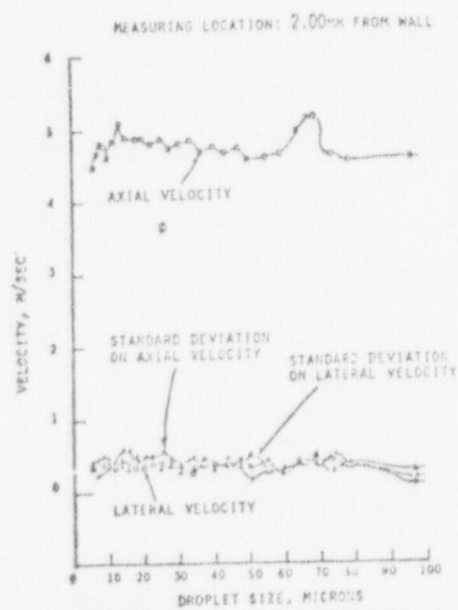


FIGURE 12. DROPLET VELOCITY DISTRIBUTIONS WITH LIQUID FILM ON WALL

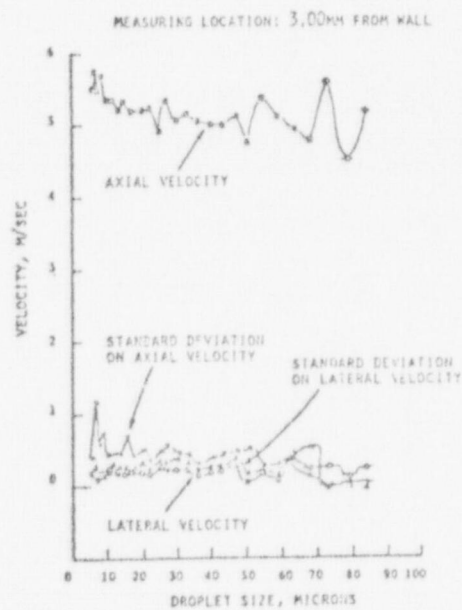


FIGURE 13. DROPLET VELOCITY DISTRIBUTIONS WITH LIQUID FILM ON WALL

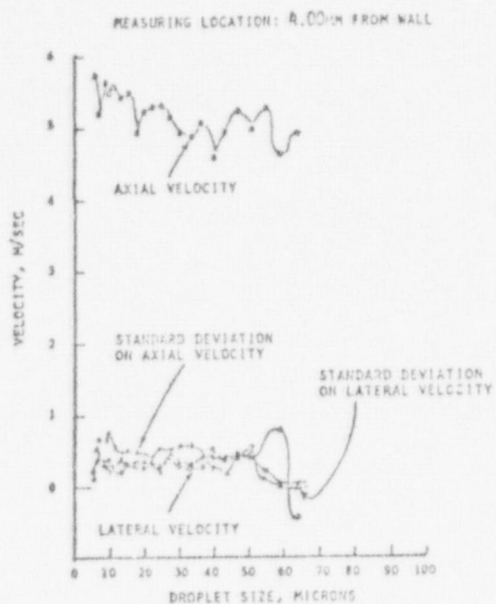


FIGURE 14. DROPLET VELOCITY DISTRIBUTIONS WITH LIQUID FILM ON WALL

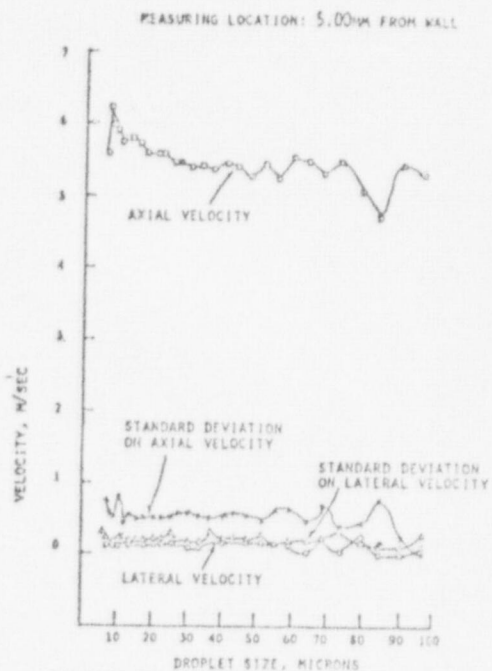


FIGURE 15. DROPLET VELOCITY DISTRIBUTIONS WITH LIQUID FILM ON WALL

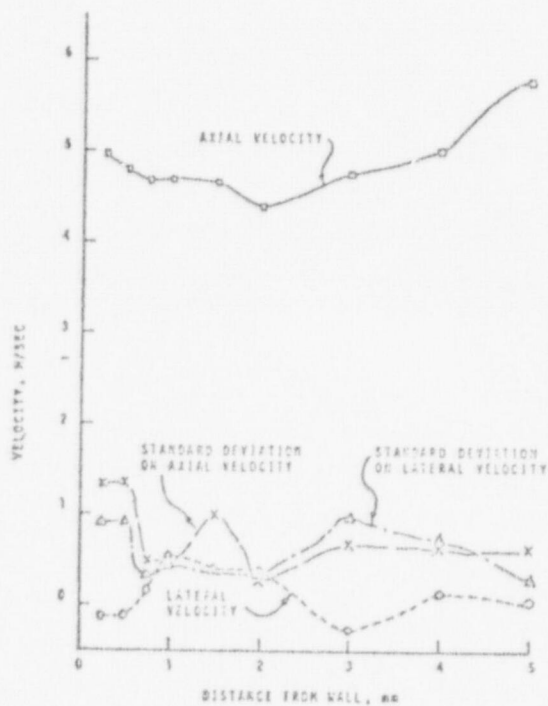


FIGURE 16. AIR VELOCITY DISTRIBUTIONS WITH LIQUID FILM ON WALL

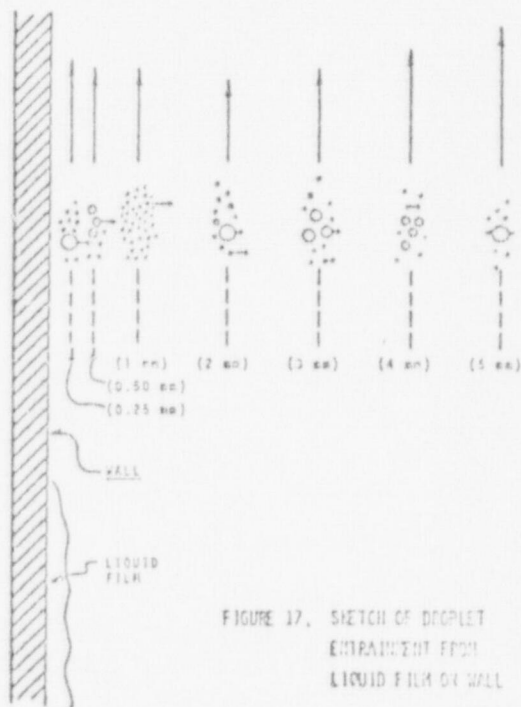


FIGURE 17. SKETCH OF DROPLET ENTRAINMENT FROM LIQUID FILM ON WALL

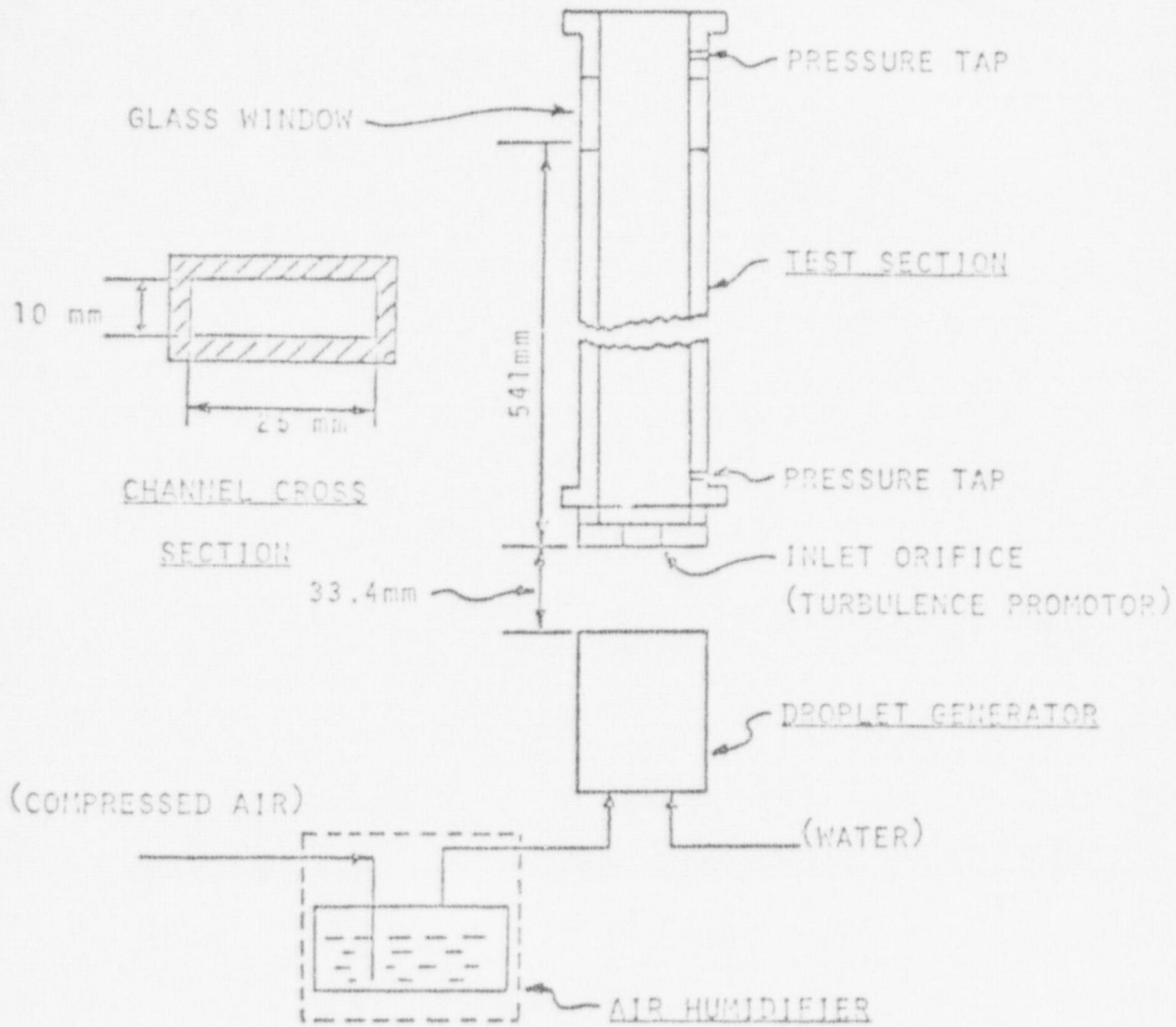


FIGURE 18. FLOW ARRANGEMENT

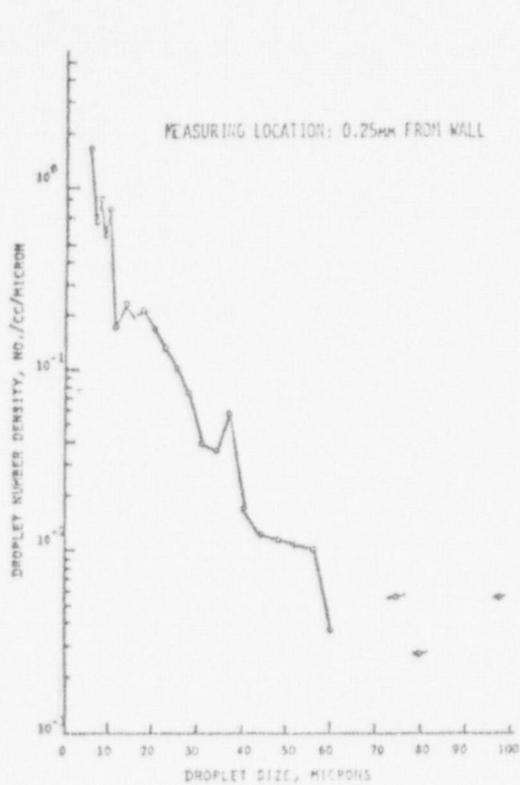


FIGURE 19. DROPLET SIZE AND NUMBER DENSITY DISTRIBUTIONS WITHOUT LIQUID FILM ON WALL

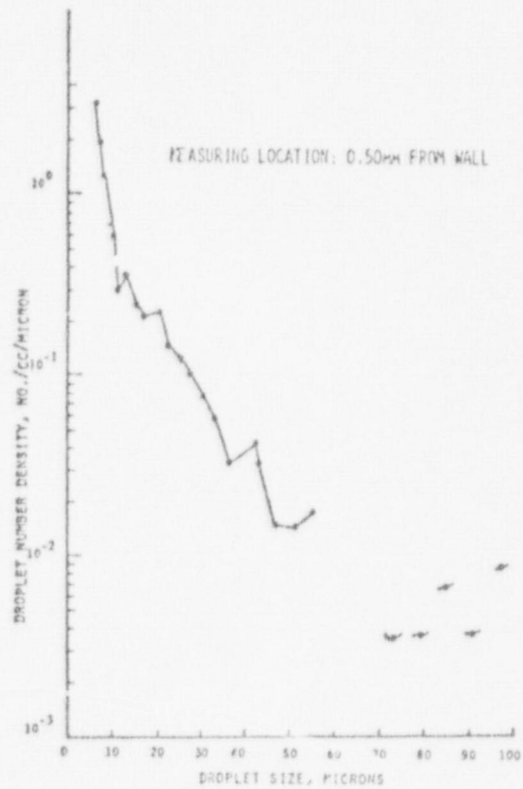


FIGURE 20. DROPLET SIZE AND NUMBER DENSITY DISTRIBUTIONS WITHOUT LIQUID FILM ON WALL

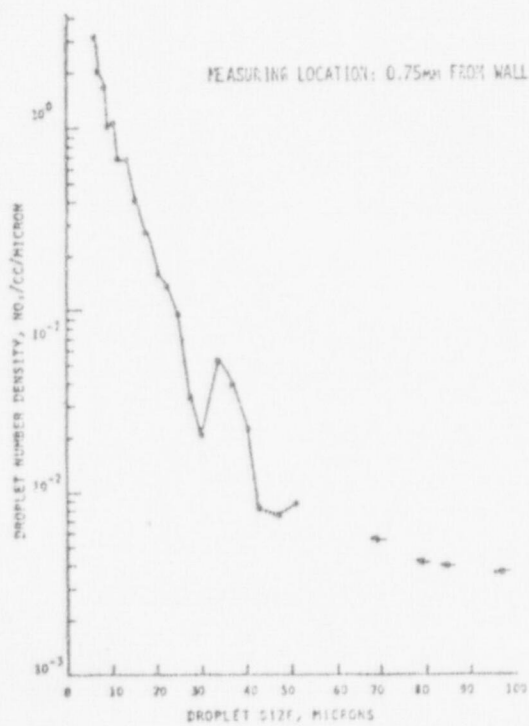


FIGURE 21. DROPLET SIZE AND NUMBER DENSITY DISTRIBUTIONS WITHOUT LIQUID FILM ON WALL

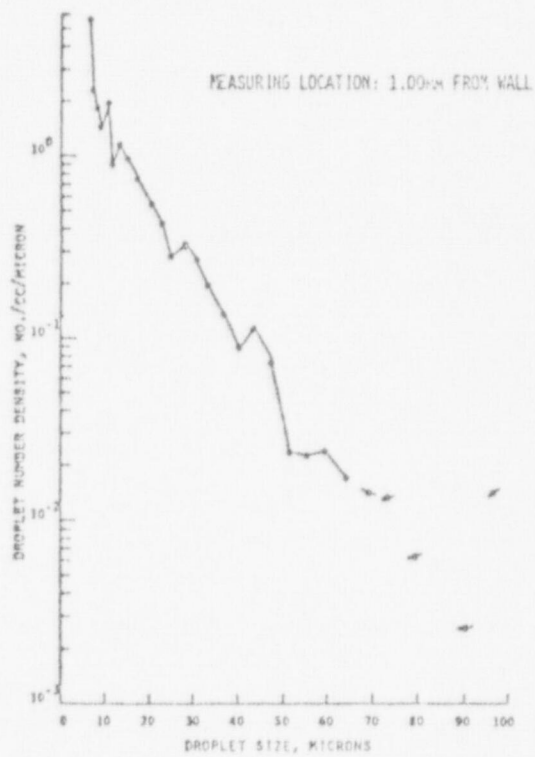


FIGURE 22. DROPLET SIZE AND NUMBER DENSITY DISTRIBUTIONS WITHOUT LIQUID FILM ON WALL

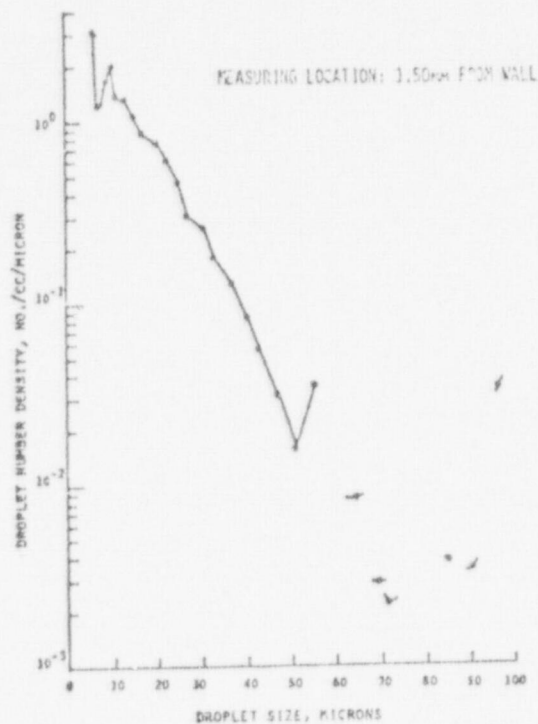


FIGURE 23. DROPLET SIZE AND NUMBER DENSITY DISTRIBUTIONS WITHOUT LIQUID FILM ON WALL

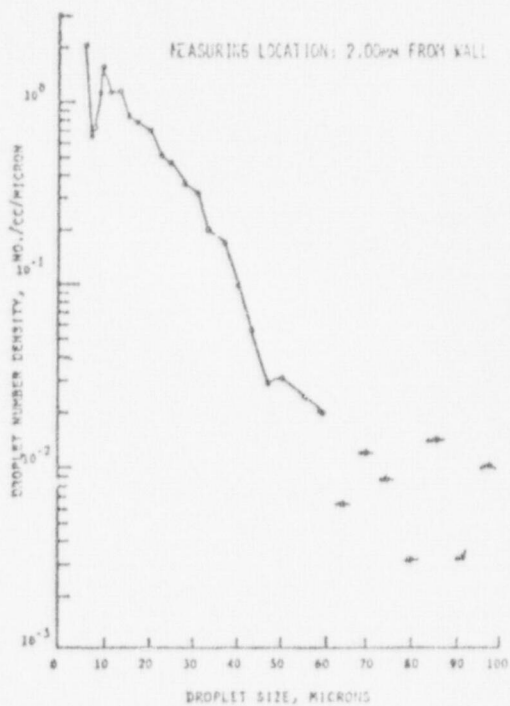


FIGURE 24. DROPLET SIZE AND NUMBER DENSITY DISTRIBUTIONS WITHOUT LIQUID FILM ON WALL

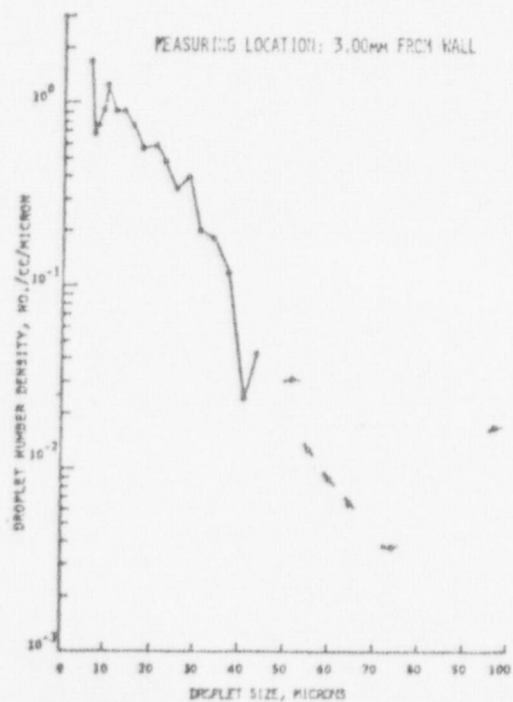


FIGURE 25. DROPLET SIZE AND NUMBER DENSITY DISTRIBUTIONS WITHOUT LIQUID FILM ON WALL

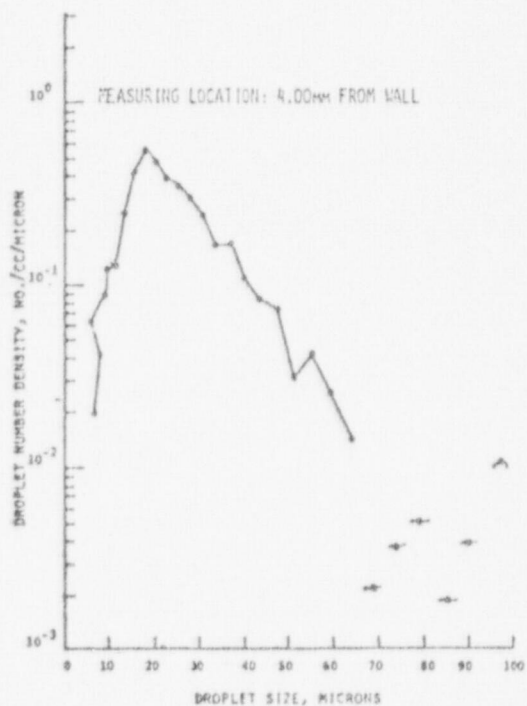


FIGURE 26. DROPLET SIZE AND NUMBER DENSITY DISTRIBUTIONS WITHOUT LIQUID FILM ON WALL

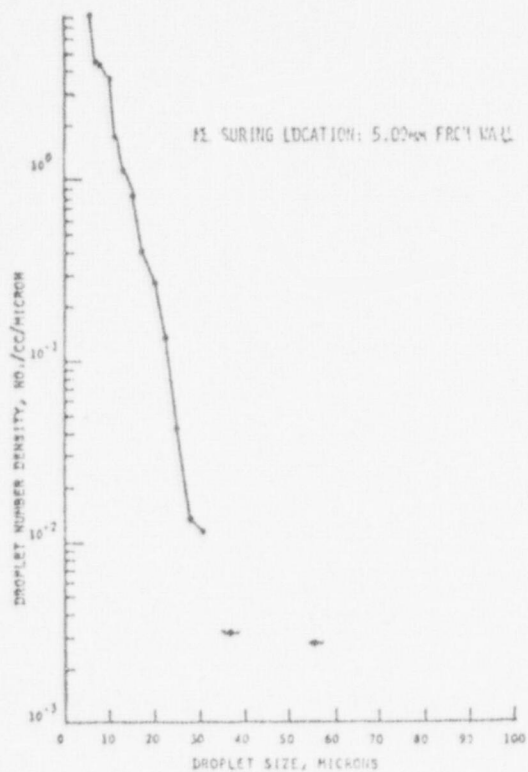


FIGURE 27. DROPLET SIZE AND NUMBER DENSITY DISTRIBUTIONS WITHOUT LIQUID FILM ON WALL

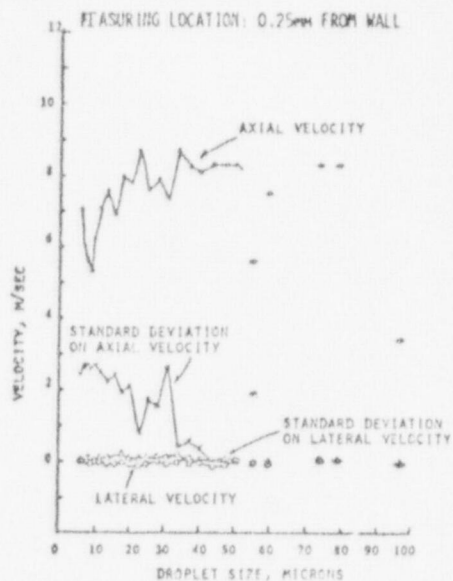


FIGURE 28. DROPLET VELOCITY DISTRIBUTIONS WITHOUT LIQUID FILM ON WALL

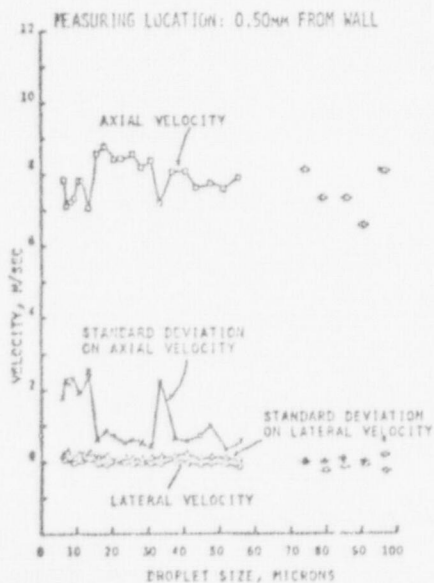


FIGURE 29. DROPLET VELOCITY DISTRIBUTIONS WITHOUT LIQUID FILM ON WALL

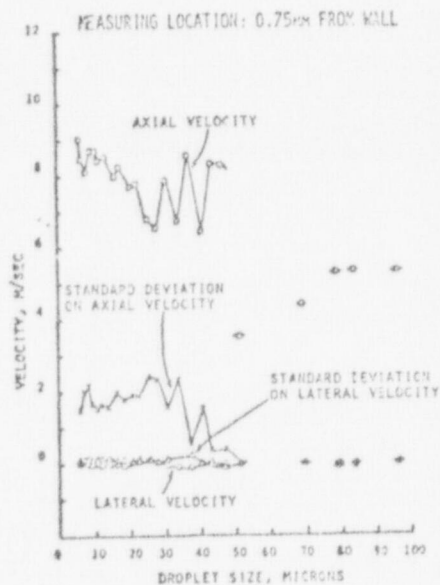


FIGURE 30. DROPLET VELOCITY DISTRIBUTIONS WITHOUT LIQUID FILM ON WALL

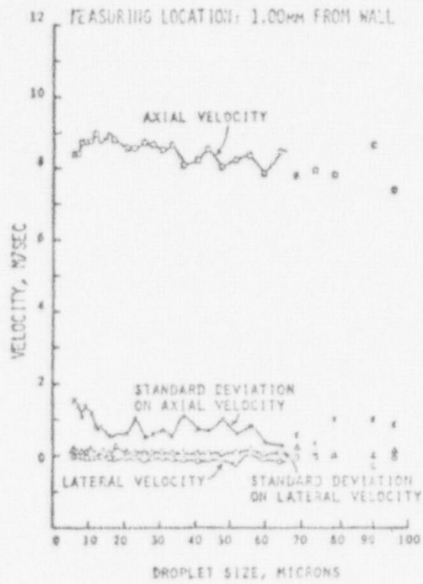


FIGURE 31. DROPLET VELOCITY DISTRIBUTIONS WITHOUT LIQUID FILM ON WALL

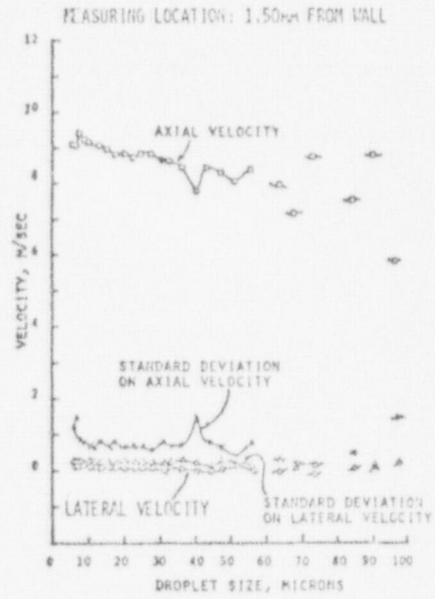


FIGURE 32. DROPLET VELOCITY DISTRIBUTION WITHOUT LIQUID FILM ON WALL

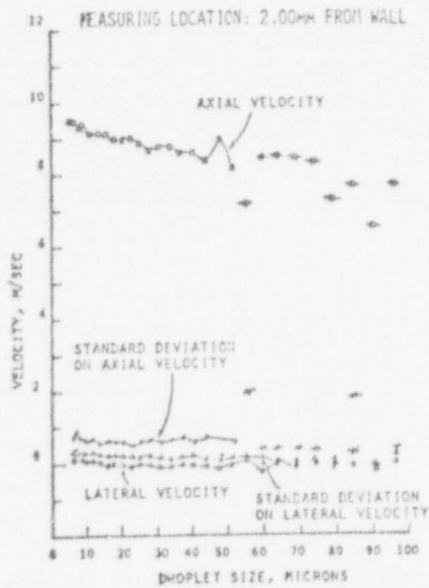


FIGURE 33. DROPLET VELOCITY DISTRIBUTIONS WITHOUT LIQUID FILM ON WALL

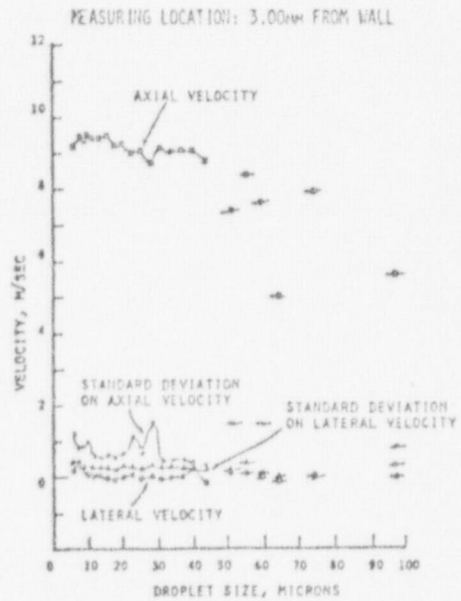


FIGURE 34. DROPLET VELOCITY DISTRIBUTIONS WITHOUT LIQUID FILM ON WALL

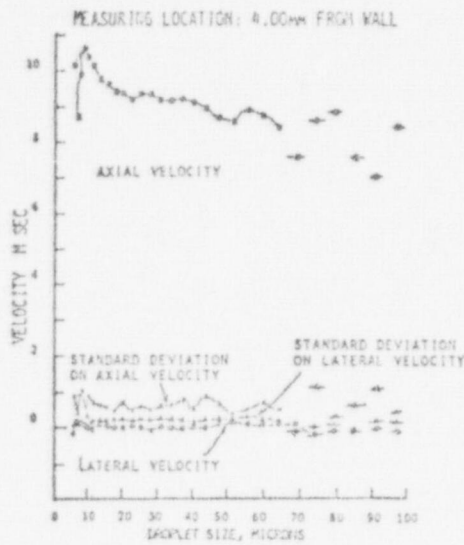


FIGURE 35. DROPLET VELOCITY DISTRIBUTIONS WITHOUT LIQUID FILM ON WALL

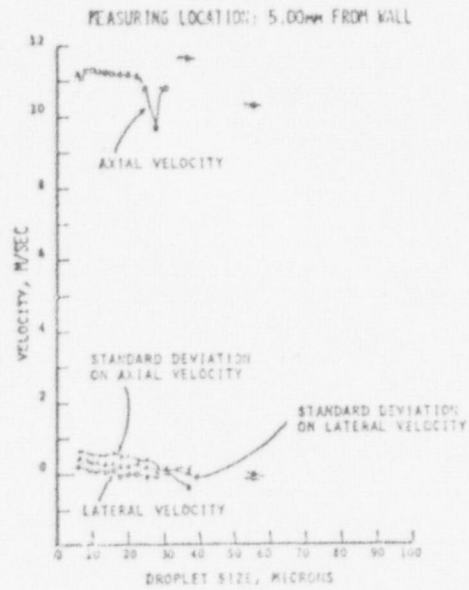


FIGURE 36. DROPLET VELOCITY DISTRIBUTIONS WITHOUT LIQUID FILM ON WALL

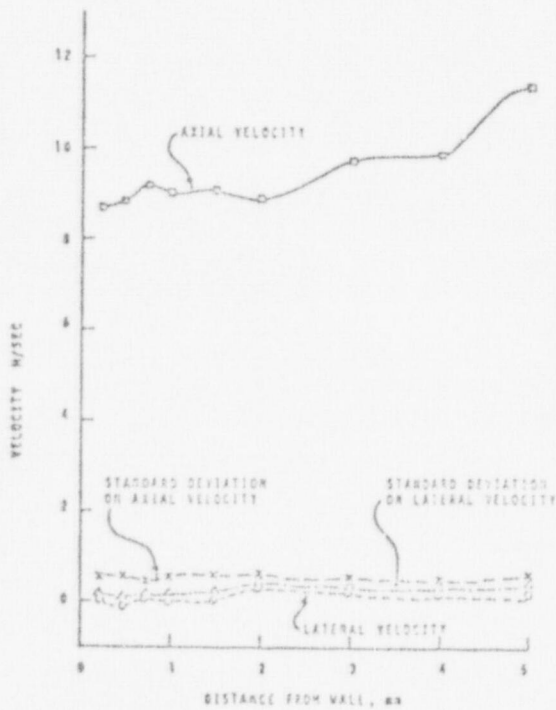


FIGURE 37. AIR VELOCITY DISTRIBUTIONS WITHOUT LIQUID FILM ON WALL

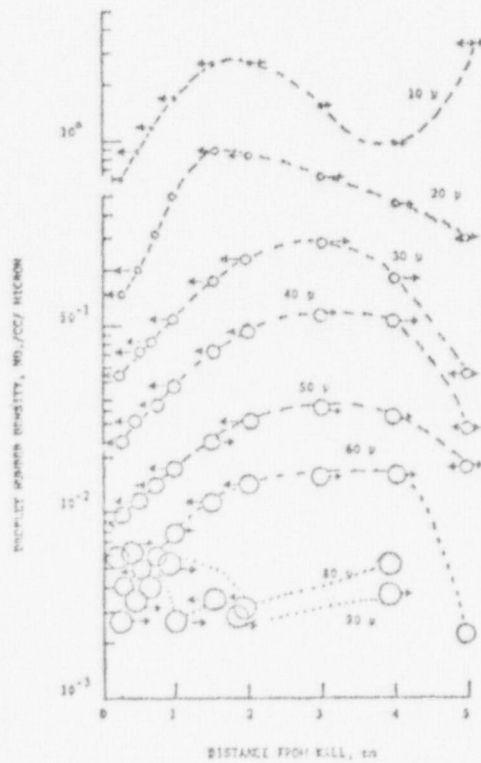


FIGURE 38. DROPLET DISTRIBUTIONS WITHOUT LIQUID FILM ON WALL

TABLE, 1.
FLOW CONDITIONS

● WITH LIQUID FILM ON THE CHANNEL WALL

AVERAGE AIR VELOCITY = 5.21 M/SEC

FLOW REYNOLDS NO. = 3,600

AXIAL PRESSURE GRADIENT = 1.32 MM OF H₂O/M

TEMPERATURE = 20°C

DROPLET SIZE RANGE : UP TO 100 μ

DISTANCE FROM THE ENTRANCE TO THE
MEASURING LEVEL : 582MM

● WITHOUT LIQUID FILM ON THE CHANNEL WALL

AVERAGE AIR VELOCITY = 9.52 M/SEC

FLOW REYNOLDS NO. = 6,600

AXIAL PRESSURE GRADIENT = 1.54 MM OF H₂O/M

TEMPERATURE = 20°C

DROPLET SIZE RANGE : UP TO 100 μ

DISTANCE FROM THE ENTRANCE TO THE
MEASURING LEVEL : 541MM

SECTION B: MODEL DEVELOPMENT

(D. S. Azbel)

AN ONE-DIMENSIONAL ANALYSIS OF THE MOTION OF SMALL LIQUID DROPLETS (10- 97 μm) IN THE FLOW OF TWO-PHASE DISPERSION IN A RECTANGULAR VERTICAL DUCT.

In the case of droplet size from 10 to 97 μm , we will assume that the motion is determined by large-scale eddies, and the gas (air) acceleration depends on the dissipation of energy, ϵ , and scale of pulsation, λ , in the form¹

$$\omega_{\lambda} \approx \frac{\epsilon_0^{2/3}}{\lambda^{1/3}} \quad (1)$$

where

$$\epsilon_0 \approx \frac{\epsilon}{\rho_g} \quad (2)$$

(ρ_g is the density of gas)

and ω_{λ} is the acceleration of large-scale eddies, and λ is the scale of these eddies. For $\rho_f \neq \rho_g$, the droplet acceleration, ω_f , will be less than the gas flow acceleration which we take to be equal to the acceleration, ω_{λ} , of large-scale eddies

$$\omega_f = \omega_{\lambda} - \omega_{\text{rel}} \quad (3)$$

The relative acceleration is

$$\omega_{\text{rel}} = \frac{u_{\text{rel}}}{\tau} \quad (4)$$

The period of droplet motion¹ is

$$\tau = \frac{d^2}{\nu} \quad (5)$$

(ν is kinematic viscosity)

and so the equation (3) becomes

$$\omega_f = \frac{\epsilon_0^{2/3}}{\lambda^{1/3}} - \frac{u_{rel}^{\nu}}{d^2} \quad (6)$$

Using dimensional analysis, we can determine the eddy period as¹

$$\tau = \frac{\lambda^{2/3}}{\epsilon_0^{1/3}} \quad (7)$$

Let us now consider the motion of droplets in a homogeneous isotropic turbulent air flow. We will use Thomson and Kirgoff's theory, in which we assume the droplets and the gas (air) as one system. Using such an approach, the problem of calculating the gas pressure on the surface of the droplets no longer arises, this being an internal system constraint only².

For the motion of a droplet in a homogeneous isotropic turbulent flow, let the gas surrounding the droplet have an acceleration, ω_g . We would determine, in this case, what the acceleration of the droplet, ω_f , will be. Neglecting gravitational forces and perturbations of the flow caused by the droplet itself, all the elements of the gas in the neighborhood of the droplet have identical accelerations, ω_g , and this acceleration is connected with a pressure drop in the direction of the acceleration vector given by³

$$\frac{\partial p}{\partial x} = \rho_g \omega_g \quad (8)$$

As a result of this pressure drop, on a droplet with the volume, V , located in the gas, there acts a force $V\rho_g\omega_g$ in the direction of the acceleration vector, but since the density ρ_f of the droplet is not equal to the density ρ_g of the gas, the acceleration ω_f of the droplet is also not equal to the acceleration of the gas and the droplet thus moves relative to the gas with an acceleration equal to $(\omega_f - \omega_g)$. For relative motion of a droplet in the gas with a non-constant velocity, the effect exerted on the droplet by the gas is given by additional term $\rho_g V_a$ added to the mass of the droplet³. Here V_a can be envisioned as a volume of liquid considered attached to the droplet and which moves with the droplet. This means that the total influence of gas motion on the droplet can be represented as an increase in its mass and, consequently, as an increase of the total system inertia. As a result of the relative motion of the droplet in the gas, a resistance is set up directed opposite to the driving force and proportional to the added mass $\rho_g V_a$, that is, equal to $\rho_g(\omega_f - \omega_g)V_a$ and so the equation of relative motion of a droplet in turbulent flow can be represented in the form

$$\rho_g[\omega_g V - (\omega_f - \omega_g)V_a] = \rho_f V \omega_f \quad (9)$$

From equation (9), we find the droplet acceleration as a function of the total gas acceleration:

$$\omega_f = \omega_g \frac{V + V_a}{V \frac{\rho_f}{\rho_g} + V_a} \quad (10)$$

Taking account of the added mass thus makes a noticeable contribution to the value of ω_f , and, for example, for particles approaching a spherical form the added mass is equal to half the mass of the displaced gas⁴. Now, substituting in equation (10), the gas acceleration, ω_λ , which is equal to ω_g from equation (1) and droplet acceleration, ω_f , from equation (6) and taking into account equation (4) and equation (9) we can rewrite the relative velocity as

$$v_{rel} \approx \left(\frac{\epsilon_0}{\nu}\right)^{1/2} \cdot a \left(\frac{V \frac{\rho_f}{\rho_g} - V}{V \frac{\rho_f}{\rho_g} + V'} \right) \quad (11)$$

At real conditions, when there is a system of discrete droplets in turbulent flow, each droplet is influenced by the other droplets which are in immediate contact with it as well as more distant, i.e. the pattern of discrete droplets' motion is to a large measure determined by their concentration⁵. For determination of this effect (constrained motion) we will use the cell model.

Let us suppose each droplet is in a center of sphere formed by adjacent droplets. With such an assumption, the problem of constrained motion may be reduced to a problem of liquid motion between two cocentric spheres.

The qualitative influence of droplets on energy spectrum, $E(N)$, to turbulent pulsations was investigated in work and was shown that addition of particles does not change the spectrum in the range wave-numbers of $N \ll N_d \sim d^{-1}$ but favors to effective extinguishing of

eddies in range of $N \gg N_d$.

In order to simplify the problem, we can speak about detachment of short-wave range, $E(N)$, starting from some characteristic wave-number N_0 ; and in general, at the range $N < N_0$ spectrum $E(N)$ does not change by adding droplets, when droplet concentration is sufficiently large, the eddies which sizes are less than diameters of droplets, are completely extinguished.

The first approximation, at sufficiently high concentration of droplets when the radius of "external" sphere becomes commensurable with a double diameter of a droplet, the motion of gas inside the sphere may be considered as laminar.

In conditions of high droplet concentration, because the droplet size is essentially less than an eddy of the scale, λ , the groups of neighboring droplets will be involved in motion--being in the same eddy of definite direction.

Consequently, the central droplet and "spherical shell", which is composed by neighboring droplets, are in motion with equal velocities; we may consider that outer shell is immovable with respect to central droplet. In this case, the following expressions for radial and tangential components of velocities relative to sphere center were proposed:

$$v_{rel}^r = \left(\frac{A}{r^3} + \frac{B}{r} + c^1 + D^1 r^3 \right) \cos\theta - v_{rel} \cos\theta \quad (12)$$

$$v_{rel}^\theta = \left(\frac{A}{2r^3} - \frac{B}{2r} - c^1 - 2D^1 r^3 \right) \sin\theta + v_{rel} \sin\theta \quad (13)$$

where

$$\left. \begin{aligned}
 A &= - \frac{v_{rel} b^3}{2-3p + 3p^5 - 2p^6} \\
 B &= \frac{v_{rel} b(2p^5 + 3)}{2-3p + 3p^5 - 2p^6} \\
 C^1 &= \frac{-v_{rel} b(2p^5 + 3)}{2-3p + 3p^5 - 2p^6} \\
 D^1 &= \frac{v_{rel} p^3}{(2-3p + 3p^5 - 2p^6)r^2}
 \end{aligned} \right\} \quad (14)$$

where:

$$p = \frac{a}{b} \quad (15)$$

(a - droplet radius; b - radius of the sphere);

taking some physically well-founded assumptions for the case when $Sc \gg 1$ expressions (12) and (13) may be reduced to the form

$$v_{rel}^{\theta} = v_{rel} \psi(p) \frac{y}{b} \sin \theta \quad (16)$$

$$v_{rel}^r = -v_{rel} \psi(p) \left(\frac{y}{b}\right)^2 \cos \theta \quad (17)$$

where:

$$y = r - b$$

Thus, constraint conditions of motion may be considered by a separate factor $\psi_1(P)$:

$$v_{rel} \sim v_{rel}^0 \psi(P) \quad (18)$$

where:

$$\psi_1(P) = \frac{3 - \frac{g}{2}p + \frac{g}{2}p^3 - 3p^6}{3 + 2p^5} \quad (19)$$

Taking into account equation (19) the relative velocity of a droplet in constrained motion may be rewritten as

$$v_{f \cdot rel} = \left(\frac{\epsilon_0}{\nu} \right)^{1/2} a \left(\frac{\Delta \rho}{\rho_f + 0.5\rho_g} \right) \psi_1(P) \quad (20)$$

As follows from equation (20) the relative velocity of a droplet in constrained motion is determined by droplet size, energy dissipation and volume content of liquid phase.

Because energy dissipation

$$\epsilon \approx v_g^3 \quad (21)$$

and particle relative velocity

$$v_{f \cdot rel} \sim v_g^{3/2} \quad (22)$$

the relative velocity of a particle may be rewritten as

$$v_{f \cdot rel} = \text{const} \left(\frac{\Delta \rho}{\rho_f + 0.5\rho_g} \right) \psi_1(P) \frac{v_g^{3/2}}{(\lambda \nu)^{1/2}} \cdot a \quad (23)$$

if we take into account the equations (18) and (19).

Because $\rho_f \gg \rho_g$ and the concentration of droplets in the gas flow is low, the equation (23) may be simplified as

$$v_{f \cdot rel} = K v_g^{3/2} \cdot a \quad (24)$$

Srinivasan and Lee measured the size and two-dimensional velocity distributions of the air in a turbulent upward flow of a

water droplet-air dispersion in a 10 mm-wide, 25 mm-deep and ~560 mm-long rectangular channel by the Laser-Doppler Anemometry technique. A comparison of equation (24) with these measurements is shown in Table 1. From this comparison, the constant K in equation (24) is thus determined as

$$K = 0.465 + 0.17 \left[\frac{1}{2} - (1 + \delta) \right], \text{ for } 1.0 \leq \delta \leq 3.0 \text{ mm}$$

and

$$K = 0.805 + 0.277 \left[\frac{1}{2} - (2 + \delta) \right], \text{ for } 3.0 \leq \delta \leq 5.0 \text{ mm.}$$

Table 1: Comparison of Measured Droplet Relative Velocity in a Rectangular Channel without Liquid Film on Wall with Corresponding Theoretical Results.

d_p (μk)	V_g (M/Sec)	V_f (M/Sec)	V_{rel}^{exp} (M/Sec)	K $(\frac{\text{Sec}^{1/2}}{\text{M}^{3/2}})$	\bar{K} $(\frac{\text{Sec}^{1/2}}{\text{M}^{3/2}})$	V_{rel}^{calc} (M/Sec)	Disc %
1	2	3	4	5	6	7	8
Measuring Location: 1.00 mm from wall							
96.76	9.00	7.48	1.52	0.582	0.463	1.210	20.39
90.62		8.70	0.30	0.123		1.133	277.66
79.24		7.90	1.10	0.514		0.928	15.64
73.96		8.08	0.92	0.461		0.925	0.54
68.96		7.86	1.14	0.612		0.862	24.39
64.21		8.53	0.47	0.271		0.803	70.85
59.69		7.87	1.13	0.701		0.746	33.98
55.40		8.39	0.61	0.408		0.693	13.60
51.32		8.29	0.71	0.512		0.642	9.58
47.45		8.00	1.00	0.781		0.593	40.70
43.77		8.53	0.47	0.398		0.547	16.38
40.28		8.25	0.75	0.883		0.504	32.80
36.96		8.03	0.97	0.972		0.462	52.37
33.80		8.64	0.36	0.394		0.423	17.50
30.79		8.55	0.45	0.541		0.385	14.44
27.95		8.71	0.29	0.384		0.349	20.34
25.24		8.78	0.22	0.323		0.316	43.64
22.66		8.61	0.39	0.637		0.283	27.44
20.22		8.63	0.37	0.678		0.253	31.62
17.89		8.80	0.20	0.414		0.224	12.00
15.68		8.94	0.06	0.142		0.196	226.66
13.59		8.79	0.21	0.572		0.170	19.05
11.60		8.99	0.01	0.032		0.145	1350.00
10.09		8.74	0.26	0.954		0.126	51.54
9.03		8.71	0.29	1.189			
8.02		8.75	0.25	1.154			
7.06		8.46	0.54	2.833			
6.14		8.45	0.55	3.318			

Table 1: Continued.

1	2	3	4	5	6	7	8
<u>Measuring Location: 1.50 mm from wall</u>							
96.76	9.08	5.77	3.31	1.250	0.550	1.456	56.00
90.62		8.72	0.36	0.145		1.364	278.00
84.78		7.49	1.59	0.685		1.276	19.76
73.96		8.72	0.36	0.178		1.113	200.00
68.96		7.10	1.98	1.049		1.038	47.58
64.21		7.91	1.17	1.009		0.966	17.41
55.40		8.40	0.68	0.449		0.834	22.60
51.32		8.06	1.02	0.726		0.772	24.29
47.45		8.36	0.72	0.555		0.714	0.83
43.77		8.41	0.67	0.559		0.659	1.69
40.28		7.81	1.27	1.152		0.606	52.27
36.96		8.48	0.60	0.593		0.555	7.30
33.80		8.64	0.44	0.476		0.509	15.60
30.79		8.59	0.49	0.582		0.463	5.44
27.95		8.78	0.30	0.392		0.421	40.00
25.24		8.76	0.32	0.463		0.380	18.69
22.06		8.65	0.43	0.694		0.341	20.70
20.22		8.75	0.33	0.596		0.304	7.79
17.89		8.82	0.26	0.531		0.269	3.54
15.68		8.93	0.15	0.350		0.236	57.30
13.59		9.02	0.02	0.054		0.204	900.00
11.60		9.08	0.00	--			
10.09		9.15	0.07	0.254		0.152	1000.00
9.03		9.21	0.13	0.526			
3.02		9.40	0.32	1.458			
7.06		9.07	0.01	0.052			
6.14		9.08	0.00	--			
<u>Measuring Location: 3.00 mm from wall</u>							
96.76	9.75	5.59	4.16	1.412	0.780	2.298	44.77
73.96		7.92	1.83	0.813		1.813	0.95
64.21		4.99	5.26	2.690		1.525	71.00
59.69		7.65	2.10	1.155		1.417	32.50
55.40		8.39	1.36	0.806		1.358	0.17
51.31		7.38	2.37	1.517		1.218	48.59
43.77		8.81	0.94	0.705		1.073	14.12
40.28		9.08	0.67	0.546		0.957	42.76
36.96		9.08	0.67	0.595		0.878	30.99
33.80		9.06	0.69	0.670		0.828	20.05
30.79		9.20	0.55	0.582		0.731	32.93
27.95		8.77	0.98	1.152		0.664	32.27
25.24		9.10	0.65	0.846		0.618	4.83
22.66		9.03	0.72	1.044		0.538	25.26
20.22		9.30	0.45	0.731		0.496	10.12
17.89		9.27	0.48	0.881		0.438	8.65
15.68		9.53	0.22	0.461		0.372	69.25
13.59		9.44	0.31	0.749		0.333	7.44
11.60		9.45	0.30	0.849		0.284	5.24
10.09		9.50	0.25	0.814		0.247	1.09

Table 1: Continued.

1	2	3	4	5	6	7	8
Measuring Location: 4.00 mm from wall							
96.76	9.87	8.52	1.35	0.450	0.528	1.584	17.35
90.62		7.10	2.77	0.986		1.484	46.44
84.78		7.67	2.20	0.837		1.388	36.91
79.24		8.94	0.93	0.378		1.297	39.50
73.96		8.68	1.19	0.480		1.211	17.56
68.96		7.67	2.20	1.029		1.129	48.68
64.21		8.52	1.35	0.678		1.051	22.13
59.69		8.83	1.04	0.562		0.977	6.03
55.40		8.98	0.89	0.518		0.907	1.91
51.32		8.72	1.15	0.723		0.840	26.94
47.45		8.79	1.08	0.734		0.777	28.06
43.77		9.05	0.82	0.604		0.717	12.61
40.28		9.21	0.66	0.528		0.659	0.08
36.96		9.33	0.54	0.471		0.605	12.06
33.80		9.27	0.60	0.572		0.553	7.77
30.79		9.30	0.57	0.597		0.504	11.56
27.95		9.44	0.43	0.496		0.458	6.42
25.24		9.46	0.41	0.524		0.413	0.79
22.66		9.32	0.55	0.555		0.371	32.55
20.22		9.46	0.41	0.654		0.331	19.26
17.89		9.48	0.39	0.703		0.293	24.89
15.68		9.70	0.17	0.350		0.257	51.00
13.59		9.85	0.02	0.047		0.222	100.00
11.00		10.25	0.38	1.056		0.190	50.00
10.09		10.44	0.57	1.822		0.165	71.00

Measuring Location: 5.00 mm from wall

55.40	11.36	10.33	1.03	0.486	0.251	0.532	48.35
36.96		11.66	0.30	0.212		0.354	17.93
30.79		10.77	0.59	0.500		0.296	49.85
27.95		9.73	1.63	1.523		0.269	83.52
25.24		10.80	0.55	0.579		0.243	56.58
22.66		11.16	0.20	0.230		0.217	8.45
20.22		11.20	0.16	0.206		0.194	20.96
17.89		11.18	0.18	0.263		0.171	4.86
15.68		11.20	0.16	0.266		0.150	6.19
13.59		11.24	0.12	0.231		0.130	8.40
11.60		11.29	0.07	0.157		0.111	59.26
10.09		11.29	0.07	0.181		0.097	38.53

References

1. Landau, L. D., Lifshitz, E. M., Fluid Mechanics, Pergamon Press.
2. Lamb, H., Hydrodynamics, Cambridge, 1932.
3. Prandtl, L., Tietjens, Hydro- and Aerodynamics, Dover Publishing Company, New York, 1957.
4. Kochin, N. E., Kibel, A. I., Roze, H. V., Teoreticheskaia Gidrodinamika (in Russian) 1955.
5. Ruchenstein, E., Chem. Eng. Sci. 19, 131 (1964).
6. Buevich, Mekhanika Zhidkosti e gasa, N2 (1970) in Russian.

NRC FORM 335 (7-77)		U.S. NUCLEAR REGULATORY COMMISSION BIBLIOGRAPHIC DATA SHEET		1. REPORT NUMBER (Assigned by DDC) NUREG/CR-0409	
4. TITLE AND SUBTITLE (Add Volume No., if appropriate) A Study of Droplet Hydrodynamics Important in LOCA Reflood, Quarterly Progress Report January 1, 1978 - March 31, 1978				2. (Leave blank)	
7. AUTHOR(S) R. S. L. Lee and D. S. Azbel				5. DATE REPORT COMPLETED MONTH: June YEAR: 1978	
9. PERFORMING ORGANIZATION NAME AND MAILING ADDRESS (Include Zip Code) State University of New York at Stony Brook Stony Brook, New York 11794				DATE REPORT ISSUED MONTH: June YEAR: 1978 b. (Leave blank) B. (Leave blank)	
12. SPONSORING ORGANIZATION NAME AND MAILING ADDRESS (Include Zip Code) U. S. Nuclear Regulatory Commission Systems Engineering Branch Washington, D. C. 20555 (Mail Stop 1130-SS)				10. PROJECT/TASK/WORK UNIT NO. 11. CONTRACT NO.	
13. TYPE OF REPORT Quarterly Technical Report			PERIOD COVERED (Inclusive dates) January 1, 1978 - March 31, 1978		
15. SUPPLEMENTARY NOTES				14. (Leave blank)	
16. ABSTRACT (200 words or less) <p>The purpose of the theoretical and experimental work reported here is to investigate the fluid mechanical and heat transfer phenomena that are believed to occur during the reflood portion of the hypothesized LOCA. Particular emphasis is placed on the fluid mechanical aspects in this report and the velocity and size distribution of the water droplets in a turbulent air flow have been simulated.</p> <p>The results of the local measurement of turbulent upward flow of a dilute water droplet-air two phase dispersion in a vertical rectangular channel are presented and a model is developed.</p>					
17. KEY WORDS AND DOCUMENT ANALYSIS			17a. DESCRIPTORS		
17b. IDENTIFIERS/OPEN-ENDED TERMS					
18. AVAILABILITY STATEMENT UNRESTRICTED			19. SECURITY CLASS (This report)		21. NO. OF PAGES
			20. SECURITY CLASS (This page)		22. PRICE \$

UNITED STATES
NUCLEAR REGULATORY COMMISSION
WASHINGTON, D. C. 20555

OFFICIAL BUSINESS
PENALTY FOR PRIVATE USE, \$300

POSTAGE AND FEES PAID
U.S. NUCLEAR REGULATORY
COMMISSION



120555028651 1 R2R4AN
US NRC
ACM TIDC DSB
MIKE ATSALINOS
016
WASHINGTON DC 20555